J. Fusion Energy manuscript No.
(will be inserted by the editor)

B.A. Grierson · M.W. Worstell · M.E. Mauel

The Turbulent Structure of a Plasma Confined by a Magnetic Dipole

Received: date / Accepted: date

Abstract We report a comprehensive statistical study of the turbulent structure of plasma confined by a dipole magnetic field. During steady state turbulence, the fluctuations exhibit a power-law spectrum, dominated by low frequencies, and a perpendicular correlation length that is a fraction of the device circumference. The structure of the turbulence is radially broad, with a zero parallel wavenumber ($k_{\|} \approx 0$), indicating interchange-like modes. Measurement of the field-aligned current density at the magnetic pole show the turbulence to be dominated by a small number of long wavelength modes with chaotic amplitudes and phases. Ensemble Fourier-based methods measure the linear dispersion and damping rates and the nonlinear power coupling rates between modes. These measurements reveal the nature of turbulence and show that fluctuation energy is, on average, transferred from the high frequency, short wavelength modes to the low frequency, long wavelength modes.

PACS PACS 52.35Mw · PACS 52.35.Ra · 52.55.Hc

B.A. Grierson

Department of Applied Physics and Applied Mathematics

Columbia University, New York, NY 10027 USA

Tel.: +1-212-854-4458, Fax: +1-212-854-8257

E-mail: bag2107@columbia.edu

1 Introduction

Turbulence drives transport in plasmas, and understanding turbulence is one of the most important challenges facing the optimization of future fusion reactors[1]. Key science priorities for fusion are understanding how magnetic field structure effects confinement, how turbulence causes transport, and how electric fields and mass flows are generated in plasmas [2]. The magnetic dipole provides a simple and important magnetic geometry for developing our understanding of plasma confinement, and it offers an attractive configuration option for magnetic fusion using advanced fuels [3]. The dipole geometry has no magnetic shear, as does the field-reversed-configuration, but confines plasma continuously at both low and high beta [4] because of plasma compressibility [5,6]. The dipole provides remarkably easy diagnostic access to the plasma, and plasma instabilities are observed to be interchange-like for both MHD centrifugal modes [7] and for kinetic MHD modes that have complex frequencies related to fast particle magnetic drifts [8]. While interchange modes may not dominate the dynamics of plasmas in regions with strong magnetic shear, strong interchange modes do appear to be the cause of filamentary "blobs" and fast plasma convection at the scrape-off-layer (SOL) of tokamaks [9].

The experiments reported here are motivated by our desire to understand plasma turbulence by first measuring both the local and global structures of the low frequency fluctuations of plasma density and electrostatic potential. We measure the local structure of the turbulence using two closely spaced probes, and we find a power-law frequency spectrum and a moderate correlation length. The global structure of the fluctuations are measured using high-speed, simultaneous recordings of the current distribution to one of the poles of the magnetic dipole. Using biorthogonal decomposition [10], we find the turbulence is dominated by a few large-scale structures with amplitudes and phases that vary chaotically in time. Finally, a possible connection between the locally-measured power-law turbulence spectrum and the large-scale global modes is discovered by computing the nonlinear energy transfer of the fluctuations using auto- and cross-bispectral analysis [11]. We find the short wavelength, higher frequency fluctuations to be linearly damped and also nonlinearly coupled to larger scale fluctuations. This corresponds to an "inverse energy" cascade and supports the view that large-scale, long-lived structures are the expected consequence of nonlinear "self-organization" of two-dimensional interchange turbulence in strongly magnetized plasma [12,13].

2 Creating Turbulent Plasma

The measurements reported here were made in the Collisionless Terrella Experiment (CTX), which confines hot plasma using a mechanically supported dipole magnet [7,8,14,15]. Plasma discharges are created and sustained with 1 kW of electron cyclotron resonance heating (ECRH) at 2.45 GHz, and these discharges achieve a turbulent steady state using multiple neutral gas injections. When gas fueling is sufficient, the plasma density increases beyond the O-mode cutoff, hot electron interchange instabilities [8] are suppressed, and quasi-steady turbulence is maintained until the termination of the microwave heating. Ample statistics are generated since discharge parameters are highly reproducible, and heating times last up to one second and are recorded at rates between $2.5-5\times10^5$ samples per second. The turbulent regime is characterized by intense fluctuations in potential and density, $\delta n/\langle n\rangle \sim 50-70\%$ near the plasma edge at $L=50-60$ cm, and less intense fluctuations, $\delta n/\langle n\rangle \sim 10-20\%$, closer to the fundamental resonance of the ECRH at $L=27$ cm.

3 Single-Point Measurements and Two-Point Correlations

Using a single floating potential probe, which is moved across the radius of the plasma in 2 cm increments, spectra averaged over hundred's of equivalent time intervals show a power-law of floating potential fluctuations across the accessible radius of the plasma (Fig. 1). The ensemble spectra are well converged over the entire discharge and at each radial location.

Two probes, with one being a reference and the other being situated in the 'downstream' direction of the plasma flow, permits measurement of the cross-correlation function, which determines the lag time and correlation amplitude between two points. The lag time is the lag at which the cross-correlation function is maximized. When two probes are on the same field line, the auto-correlation functions and cross-correlation function are identical. There is no variation along a field line, or $k_\parallel \approx 0$, indicating the interchange nature of the fluctuations. When two probes are separated azimuthally by $\Delta\varphi \sim 9^\circ$ (8 cm), the normalized cross-correlation amplitude remains relatively large, $\sim 90\%$, and the lag time between the signals is very small, and positive. This is representative of the average $\mathbf{E}\times\mathbf{B}$ flow of the plasma in the electron diamagnetic drift direction. When the correlation is measured between four widely-spaced probes, with separations of $\Delta\varphi \in \{9^\circ, 90^\circ, 180^\circ\}$, the decrease in cross-correlation amplitude determines the correlation length. This is found to be ≈ 45 cm, equivalent to $\Delta\varphi \sim 50^\circ$, or 14% of the device circumference. Finally, the dominate

fluctuation and mode number of the fluctuations are extracted from the squared cross-coherence and cross-phase [16] calculated using ensemble Fourier statistics. Fig. 2 indicates two modes exist in the plasma, at $f \sim 1-2$ kHz, and $f \sim 3-4$ kHz that correspond to the lowest two azimuthal mode numbers, $m = 1, 2$. Additionally, the mode structure is found to be radially broad, existing across the radial width of the plasma, with the strongest coherence nearest the heating zone.

4 Global Imaging of Plasma Dynamics

The CTX device is outfitted with a unique array of 96 gridded particle detectors[15] situated at the pole of the dipole magnet. The detectors are spaced azimuthally with separation of $\Delta\varphi = 15^\circ$ and radially span the plasma at eight locations. All detectors are placed at nearly the same magnetic field strength, $B \approx 2$ kG, and detect currents from flux-tubes having equivalent magnetic flux but strongly varying volumes,$\delta V \sim 1/\psi^4 \sim L^4$. When the detectors are biased negatively, ion current is collected in relation to the flux tube integrated density, $N = \int ds\, n/B = \langle n \rangle \delta V$. Fluctuations of the ion polar current are strongly correlated, with zero-lag time and equivalent spectral characteristics, with the fluctuations of a probe's ion saturation current when placed on the same field-line as a polar detector.

The global structure of the turbulence becomes apparent when the ion current at a particular radius is viewed as a function of azimuthal angle and time. Fig. 3 shows a color contour plot of the ion current, and the diagonal bands of current indicate low m, rotating structures. Fourier decomposition at each sample time shows that the dominate mode varies randomly in time. The lower half of Fig. 3 shows the times when each of $m \in \{1, 2, 3, 4, 5\}$ have the largest Fourier amplitude.

When data at all radii and azimuths are analyzed collectively, the turbulence can be decomposed into orthogonal spatial and orthogonal temporal modes with the Singular Value Decomposition (SVD), called "biorthogonal decomposition" [10]. No pre-defined basis functions are used for the decomposition, and the spatial structures of the modes are are extracted from the data.

Fig. 4 shows the biorthogonal decomposition of the ion current fluctuations for a relatively short, 8 ms, period during steady turbulence. The dominant spatial modes are found to rotate, be well-ordered from small to large m, and have relatively simple, radially broad structures. The mode functions come in pairs, azimuthally shifted by $\pi/2$, indicating the direction of rotation. The temporal mode functions, in contrast to the spatial

functions, show a very complex, and chaotic behavior. Each exhibits a power-law frequency spectrum, which peaks at low frequency. The temporal functions associated with the $m = 1$ spatial functions, peak at 2 kHz, and the temporal functions for the $m = 2$ mode peak at 4 kHz, indicating both modes rotate together.

The turbulent frequency spectrum of any individual polar detector can be represented using only a small number of spatial mode functions. The Fourier spectra of both the localized ion current measurement and the spectrum reconstructed using only the dominate modes, $m = 1, 2, 3, 4$, and the mean component. Both exhibit the same power-law dependence at high frequencies (similar to Fig. 1, except the power-law differs by the expected relationship between potential and density fluctuations.) The nature of interchange turbulence appears well-described by "rigid" spatial modes with complex temporal variations.

5 Bispectral Analysis Indicates that Power is Transferred from Small to Large Scales

The fluctuation power transfer as a function of frequency can be estimated statistically by measuring moments of a nonlinear wave-kinetic equation having both a linear and quadratic, three-wave, nonlinear coupling [11]. Determination of the nonlinear coupling coefficient and nonlinear power transfer function requires calculation of the auto and cross-bispectrum, as well as the fourth-order moment. Average spectral quantities require hundreds to thousands of realizations of each time-series for the phase and bispectra to converge. The spectra are therefore statistically robust, and represent the nature of the turbulent quantities on a long-time, average sense. Fig. 5 shows the result of these calculations. We find a linear relationship between frequency and wavenumber, indicative of plasma rotation, Ω, as discussed previously. Additionally, the high frequency modes are strongly damped, with damping that scales as $1/k \sim f/\Omega L$ and reaches a maximum near $f \sim 100$ kHz when $k \sim 1/\rho_i$, the inverse ion gyroradius. The power transfer can be then be estimated for the range of frequencies with known linear dispersion. As is also shown in Fig. 5, fluctuation energy is observed to flow from small scales to the scales represented by the weakly damped global modes.

6 Summary

We report the first comprehensive measurements of the structure of plasma turbulence in a dipole-confined plasma. The azimuthal decorrelation length of the turbulence is measured to be a fraction of the device circumference, and the observed modes are determined to be interchange-like, with $k_{\|} \approx 0$. Correlation and

coherence analysis provides measurement of the mode structure of floating potential fluctuations in the bulk plasma, and determines the modes structure to be dominated by $m = 1, 2$, with the strongest coherence near the heating location. Based on the imaging diagnostic at the magnetic pole, the density fluctuations are also found to be dominated by low m-numbers. The nonlinear power transfer between modes indicates that three-wave interaction couples small scales, and causes an "inverse-cascade" to large scale structures. The fluctuations of these large structures are associated with low frequency, large scale convective cells, which mixes plasma across field lines and are known to cause fluctuation-induced transport. Measurement of the transport associated with these convective motions are subject to ongoing research.

Acknowledgements Supported by DOE/SF Partnership Grant DE-FG02-00ER54585.

References

1. E. Doyle, W. Houlberg, Y. Kamada, V. Mukhovatov, T. Osborne, A. Polevoi, G. Bateman, J. Connor, J. Cordey, T. Fujita, Nucl Fusion **47**, S18 (2007)
2. C. Baker, S. Prager, M. Abdou, L. Berry, R. Betti, V. Chan, D. Craig, J. Dahlburg, R. Davidson, J. Drake, R. Hawryluk, D. Hill, A. Hubbard, G. Logan, E. Marmar, M. MAUEL, K. McCarthy, S. Parker, N. Sauthoff, R. Stambaugh, M. ULRICKSON, J.V. Dam, G. Wurden, M. Zarnstorff, S. Zinkle, J Fusion Energ **24**(1-2), 13 (2005). DOI 10.1007/s10894-005-6922-z. URL http://www.springerlink.com/content/u1858796586417x6/
3. J. Kesner, D. Garnier, A. Hansen, M. MAUEL, L. Bromberg, Nucl Fusion **44**(1), 193 (2004). DOI 10.1088/0029-5515/44/1/021
4. D. Garnier, A. Hansen, M. Mauel, E. Ortiz, A. Boxer, J. Ellsworth, I. Karim, J. Kesner, S. Mahar, A. Roach, Phys Plasmas **13**(5), 056111 (2006). DOI 10.1063/1.2186616
5. M. Rosenbluth, C. Longmire, Ann. Phys **1**(2), 120 (1957)
6. T. Gold, J. Geophys. Res. **64**(9), 1219 (1959)
7. B. Levitt, D. Maslovsky, M. Mauel, Phys Rev Lett **94**(17), 175002 (2005). DOI 10.1103/PhysRevLett.94.175002
8. B. Levitt, D. Maslovsky, M. Mauel, Phys Plasmas **9**(6), 2507 (2002). DOI 10.1063/1.1475999
9. S. Krasheninnikov, Physics Letters A **283**(5-6), 368 (2001). DOI 10.1016/S0375-9601(01)00252-3. URL http://dx.doi.org/10.1016/S0375-9601(01)00252-3
10. T. de Wit, A. Pecquet, J. Vallet, R. Lima, Phys Plasmas **1**, 3288 (1994)
11. H. Xia, M.G. Shats, Phys Plasmas **11**(2), 561 (2004). DOI 10.1063/1.1637607
12. A. Hasegawa, Advances in Physics **34**(1), 1 (1985)
13. O.E. Garcia, N.H. Bian, V. Naulin, A.H. Nielsen, J.J. Rasmussen, Phys. Scr. **T122**, 104 (2006). DOI 10.1088/0031-8949/2006/T122/014

14. D. Maslovsky, B. Levitt, M. Mauel, Phys Rev Lett **90**(18), 185001 (2003). DOI 10.1103/PhysRevLett.90.185001

15. B. Levitt, D. Maslovsky, M. Mauel, J. Waksman, Phys Plasmas **12**(5), 055703 (2005). DOI 10.1063/1.1888685

16. M.J. Burin, G.R. Tynan, G.Y. Antar, N.A. Crocker, C. Holland, Phys Plasmas **12**(5), 052320 (2005). DOI 10.1063/1.1889443

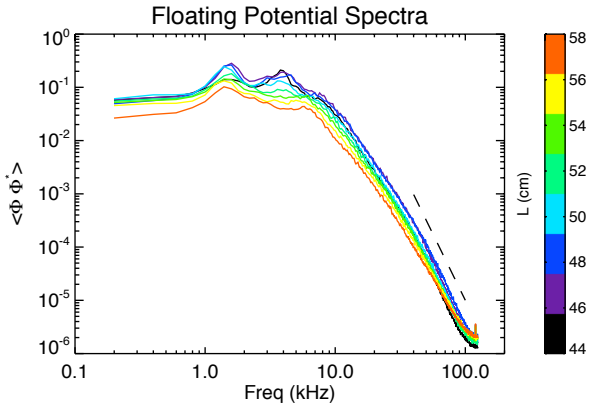

Fig. 1 The ensemble spectrum floating potential spectrum taken across the accessible plasma radius. The power law is f^{-4} near the plasma edge, and f^{-5} closer to the heating zone. The dashed f^{-5} is added to guide the eye.

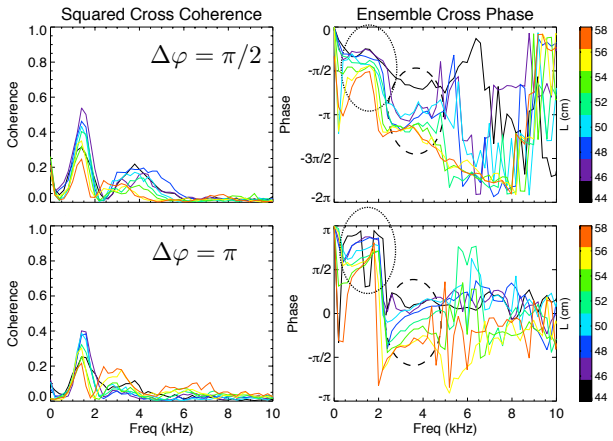

Fig. 2 Squared ensemble cross-coherence and cross-phase for probes separated azimuthally by $\Delta\varphi = \pi/2$ and π. The short dashes display an $m = 1$ mode, where $\langle\alpha\rangle \approx \Delta\varphi$, and the long dashes display an $m = 2$ mode where $\langle\alpha\rangle \approx 2\Delta\varphi$

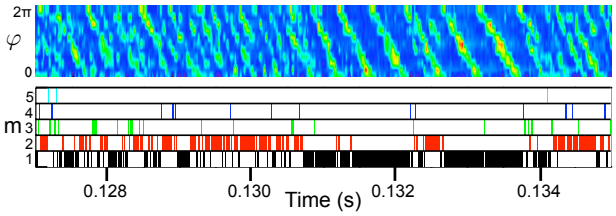

Fig. 3 Contour plot of density $n(t,\varphi)$ and m-number evolution showing that the fluctuations are dominated by low azimuthal mode numbers.

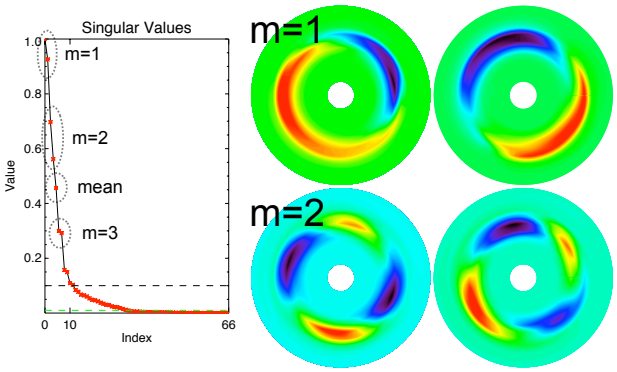

Fig. 4 The singular values and spatial mode functions calculated from the bi-orthogonal decomposition.

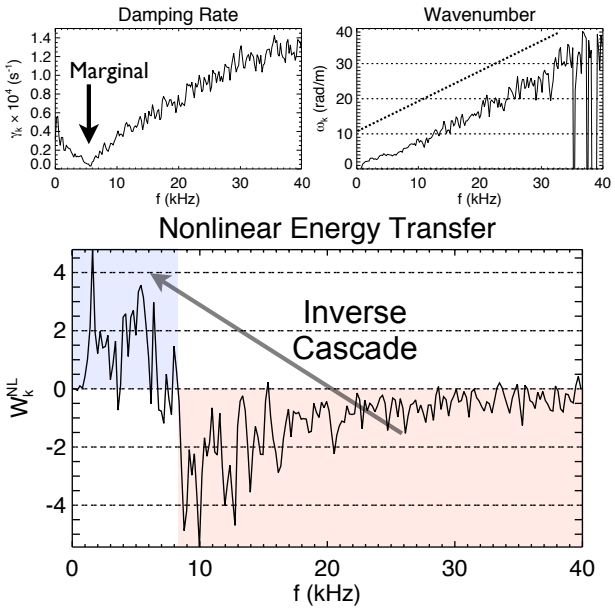

Fig. 5 Wavenumber, growth rate, and nonlinear spectral energy transfer for two floating potential probes separated azimuthally by 9°. The dispersion is linear through 35 kHz and damping increases above 5 kHz. Power is transferred nonlinearly from high to low frequencies (wavenumbers).